

High-Throughput Screening of Dense Boron Nitride Structures from Structural Templates

Yongheng Wang,[†] Yongzhe Guo,[†] Chunbo Zhang, and Enlai Gao^{*†}



Cite This: *J. Phys. Chem. C* 2025, 129, 5728–5735



Read Online

ACCESS |



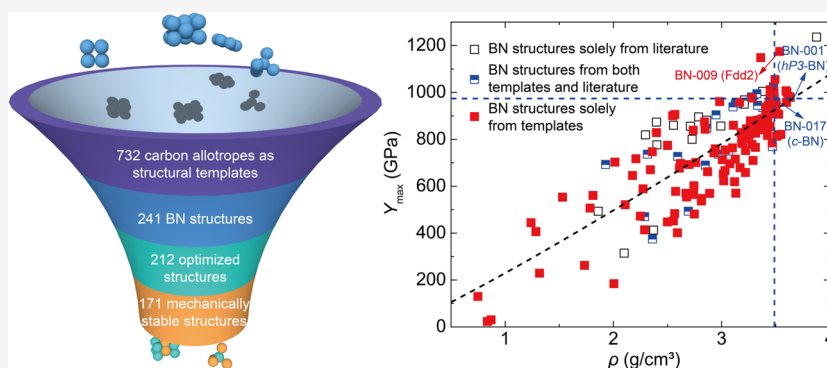
Metrics & More



Article Recommendations



Supporting Information



ABSTRACT: Considerable effort has been devoted to searching for high-performance boron nitride (BN) structures due to their promising applications competing with diamond. However, this search remains a significant challenge due to the exceedingly complex energy landscape of BN. Considering that most BN structures have a structure analogous to that of carbon, such as cubic BN to diamond, hexagonal BN to graphite, and that far more carbon allotropes than BN structures have been reported, we here collected 732 literature-reported carbon allotropes as structural templates to direct the discovery of BN structures. First-principles calculations indicate that 171 BN structures constructed from the carbon templates are mechanically stable, among which 139 are newly found and 32 have been reported. A literature survey shows that the number of known mechanically stable BN structures has more than tripled, indicating that our template-directed search dramatically extends the family of BN structures. Most interestingly, 15 mechanically and thermodynamically stable BN structures have a density higher than *c*-BN, and 13 of them are newly found, including the stiffest and strongest BN structures. Finally, the mechanisms and possible synthesis of high-performance BN structures are discussed.

INTRODUCTION

Light main group elements (B, C, N, *etc.*) that can form strong covalent bonds and possess high valence electron density are considered the most promising candidates for high-performance solids.^{1–5} Among these elements, carbon allotropes, including carbon nanotubes, graphene, and diamond, have been extensively studied because of their impressive mechanical properties.^{1–3} For instance, diamond has been long known as the hardest material and is widely used for cutting tools.⁶ However, the easy reaction of diamond with ferrous metals limits the application. As a structure analogous to diamond and the second hardest material, cubic boron nitride (*c*-BN) has excellent chemical resistance to Fe-, Co-, and Ni-containing materials.^{7,8} Compared to diamond, BN's chemical resistance makes it an ideal choice for cutting and drilling tools, as *c*-BN can cut all ferrous metals, including superalloys.^{9,10} Additionally, BN outperforms diamond in thermal stability and oxidation temperatures, making it a promising material for a wide range of applications.¹¹ BN is increasingly being used in advanced electronic and optoelectronic devices. Its potential as

an environmentally friendly and cost-effective material for next-generation thermoelectric devices further highlights BN's growing importance in sustainable technologies.^{12,13} Hence, ultrahigh-performance BN structures are promising to compete with diamond in industrial applications.

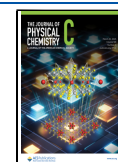
Driven by such promising uses competing with diamond, significant efforts have been devoted to the discovery of high-performance BN structures over the past decades. Since Wentorf and Bundy first reported the transformation of hexagonal BN (*h*-BN) to *c*-BN and wurtzite BN (*w*-BN) at high pressures in the 1950s and 1960s,^{14–16} the prediction, synthesis, and characterization of BN structures have been

Received: December 21, 2024

Revised: February 24, 2025

Accepted: February 27, 2025

Published: March 7, 2025



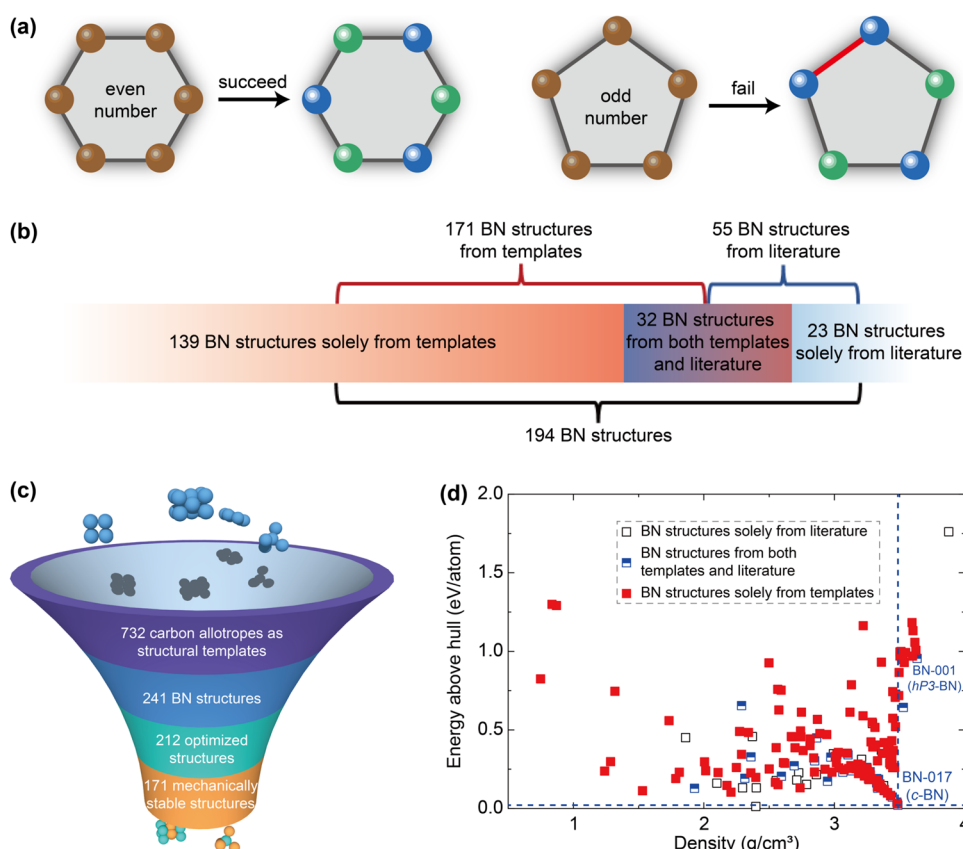


Figure 1. Screening of BN structures. (a) Illustration of atomic replacement from carbon templates, (b) mechanically stable BN structures obtained from our screening and literature, and (c) screening of mechanically stable BN structures. (d) Energies above hull for 194 mechanically stable BN structures from templates and literature.

stimulated.^{17–21} First-principles calculations provide a powerful tool for materials discovery. For instance, Kuzubov et al.²² predicted that *hP3*-BN has the highest density up to 3.66 g/cm³, and Xiong et al.²³ predicted that *Pm3n*-BN has the highest tensile strength up to 121 GPa. Furthermore, the development of structure prediction techniques, e.g., Crystal structure AnaLYsis by Particle Swarm Optimization (CALYPSO) code,²⁴ has accelerated the discovery of BN structures. By employing a microhardness model,^{25,26} Li et al.²⁷ predicted that *Pbca* (60 GPa), *Z'*-BN (60 GPa), *M*-BN (59 GPa), and *BC₈*-BN (57 GPa) exhibit hardness comparable to *c*-BN (63 GPa) and *w*-BN (63 GPa). Meanwhile, Zhou et al.²⁸ predicted that the bulk moduli of *bct*-BN (379 GPa), *bct₂W₁* (383 GPa), *bct₁W₁* (388 GPa), and *bct₂W₂* (388 GPa) are comparable to *c*-BN (404 GPa) and *w*-BN (403 GPa). These predictions provide guidelines for the experimental syntheses of BN structures.

Most BN structures have a structure analogous to that of carbon, such as *c*-BN to diamond, and *h*-BN to graphite. Despite the progress made in the discovery of BN structures, the number of known BN structures remains significantly smaller than carbon allotropes. Our literature survey shows that only 55 unique mechanically stable BN structures have been reported, whereas the Samara Carbon Allotrope Database (SACADA) has collected 703 known carbon allotropes²⁹ by April 2023. The most stable stoichiometric ratio of BN structures is B:N = 1:1,³⁰ and the B–N bonds in BN structures exhibit bonding characteristics similar to those of C–C bonds in carbon. Considering this fact, utilizing existing carbon

allotropes as structural templates holds significant potential to accelerate the discovery of BN structures.³¹

In this work, 732 carbon allotropes reported in the literature are used as templates for constructing BN structures. Screening based on first-principles calculations yields 171 mechanically stable BN structures, including 139 new and 32 known BN structures. To the best of our knowledge, the number of known stable BN structures has more than tripled, increasing from 55 to 194. Most interestingly, 15 mechanically and thermodynamically stable BN structures from templates have a density higher than *c*-BN, and 13 of them are newly found, including the stiffest BN-009 (*Fdd2*). Tensile tests show that the densest BN-001 (*hP3*-BN) has the highest recorded tensile strength. The mechanisms and possible synthesis of high-performance BN structures are discussed.

METHODS

To investigate the stabilities and mechanical properties of BN structures, first-principles calculations based on the density functional theory (DFT) were performed by using the Vienna *Ab-Initio* Simulation Package (VASP).³² The Perdew–Burke–Ernzerhof parametrization of the generalized gradient approximation was used for the exchange–correlation functional.³³ An energy cutoff of 520 eV was used, and a *k*-point mesh with a density of about 50 Å (the product of each lattice constant and the corresponding number of *k*-points) for structural optimization and about 33 Å for elasticity tensors calculation was used for Brillouin zone sampling.³⁴ All structures were fully relaxed using a conjugate gradient algorithm with a

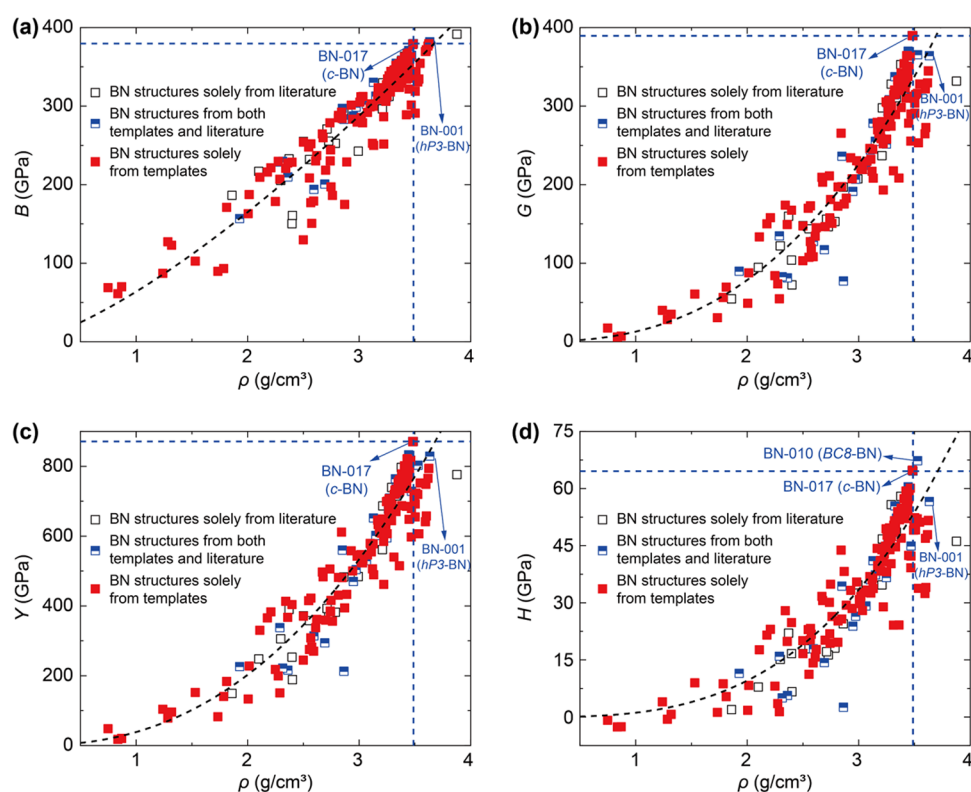


Figure 2. Performance of BN structures. (a) Bulk moduli, (b) shear moduli, (c) Young's moduli, and (d) Vickers hardness vs densities for 194 BN structures.

stringent convergence criterion of the force on each atom (10^{-3} eV/Å). In *ab initio* molecular dynamics (AIMD) simulations, an energy cutoff of 400 eV was used for a balance between computational accuracy and cost. The AIMD simulations were performed in a supercell (no less than 48 atoms) in the canonical ensemble using the Andersen thermostat.³⁵

RESULTS AND DISCUSSION

Screening of Stable BN Structures. Numerous carbon allotropes have been reported in the past decades. Hoffmann et al.²⁹ gathered together the known carbon allotropes and indexed them in the SACADA. Meanwhile, Zhang et al.³⁶ recently discovered numerous superdense carbon allotropes. High-throughput screening methods have been widely used to explore novel materials.^{37–43} These methods provide effective ways to explore mechanically and thermodynamically stable structures. Accordingly, we extracted 732 carbon structures from the SACADA²⁹ and Zhang's work³⁶ as templates for constructing BN structures. Subsequently, all the carbon atoms in these carbon templates were replaced with boron and nitride atoms, and the resultant structures without stable stoichiometric ratio of BN structures (B:N = 1:1) were filtered out (Figure 1a). Considering the computational efficiency, structures with more than 40 atoms in the primitive cell were further filtered out. As a result, 241 BN structures were retained for further structural optimization using first-principles calculations. Duplicate checking was then performed on these optimized structures using symmetry comparison, local atomic geometries, and structural mapping techniques to ensure uniqueness.⁴⁴ Additionally, BN structures with low-dimensional building blocks were removed using the topology-

scaling algorithm proposed by Ashton et al.⁴⁵ Such screening yields 212 three-dimensional energy-optimized BN structures. To evaluate their mechanical stabilities, elasticity tensors were calculated for these 212 structures using the strain–stress method.⁴⁶ The elasticity tensors for 171 structures are positive-definite, indicating their mechanical stabilities. The screening processes are illustrated in Figure 1b,c.

A literature survey identified 60 unique BN structures from experiments and computations. To ensure consistency, we optimized these structures and assessed their mechanical stabilities using first-principles calculations. Our calculations show that 55 of the BN structures reported in the literature are mechanically stable. Upon structural checking,⁴⁴ we found that 32 mechanically stable BN structures obtained from templates were also reported in the literature, which were named “BN structures from both templates and literature” (Figure 1b). The remaining 23 mechanically stable BN structures were solely reported in the literature, which were named “BN structures solely from literature”. This indicates that 139 BN structures obtained from templates are newly found compared to the 55 structures reported in the literature (Figure 1b). These 139 newly found BN structures were named “BN structures solely from templates”. These results demonstrate that template-directed search dramatically extends the family of BN structures, since the number of known stable BN structures has more than tripled (from 55 to 194). All these 194 BN structures are provided in the Supporting Information (Table S1). Formability is important for practical applications, which can be measured by energies above hull. The energies above hull of BN structures were calculated as the energy difference between the energy for a BN structure and that of the lowest energy BN (*h*-BN). The calculated energies above hull of these

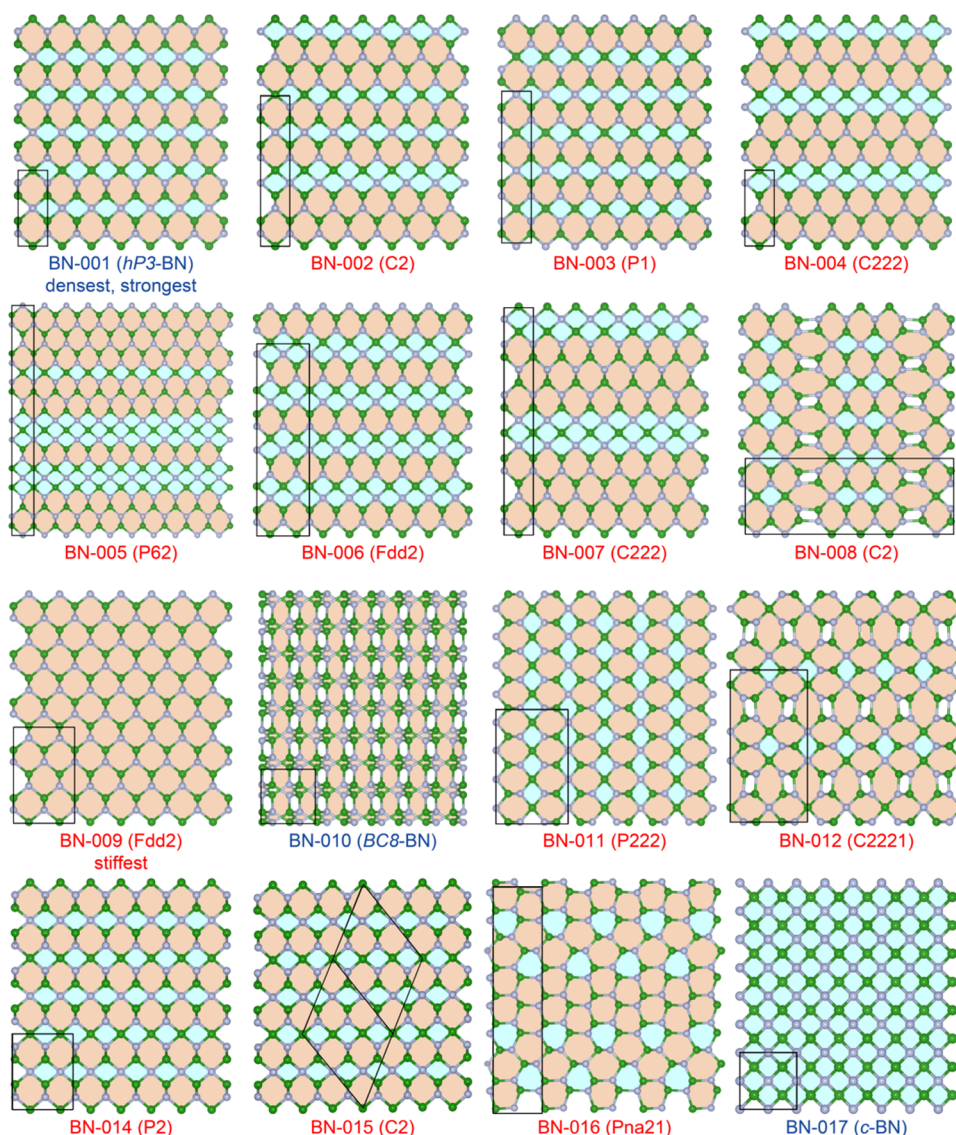


Figure 3. Stable superdense BN structures compared to *c*-BN. BN structures not reported in the literature are marked with their space groups, and the literature-reported structures are marked with their names in the literature.

194 mechanically stable BN structures are shown in Figure 1d and Table S1.

Mechanical Performance of BN Structures. We investigated the mechanical properties of these BN structures. Based on the theory of elasticity, we calculated the Voigt-Reuss-Hill average elastic moduli of BN structures.⁴⁷ Unless otherwise noted, the elastic moduli mentioned below are all based on the Voigt-Reuss-Hill averaging scheme. The bulk modulus (*B*), shear modulus (*G*), and Young's modulus (*Y*) can be derived from the elasticity tensor of a material (Figure 2a–c and Table S1). Elastic moduli not only characterize the resistance of a material to elastic deformation but also have a close correlation with other important properties. For example, Vickers hardness of a material can be correlated with the bulk modulus and shear modulus as $H = 2(G^3/B^2)^{0.585} - 3$.⁴⁸ Therefore, the hardness of these BN structures can be further estimated from their elastic moduli (Figure 2d and Table S1). As a validation, our calculated bulk modulus (380 GPa), shear modulus (390 GPa), Young's modulus (871 GPa), and Vickers hardness (65 GPa) of *c*-BN, agree well with the literature-reported corresponding values (376, 382, 856, and 65 GPa,

respectively).^{49,50} We identified several BN structures with novel superhard properties. These structures exhibit Vickers hardness values comparable to recently reported BN structures, such as the *Pm* BN reported by Fan et al.⁵¹ and *O*-BN reported by Huang et al.⁵² The hardness of these new BN structures could be further enhanced through nanostructuring, such as nanograin and nanotwinned microstructures, providing a general pathway for designing advanced materials with exceptional thermal stability and mechanical properties.^{53,54}

We further explored the correlations between the densities and the mechanical properties. These results show that the correlation coefficients (R^2) of densities with *B*, *G*, *Y*, and *H* are as high as 0.88, 0.88, 0.89, and 0.81, respectively (Figure 2). Meanwhile, the correlation of the highest Young's modulus with the density is also strong (Figure S1). These strong correlations between the densities and the mechanical properties suggest that high density can serve as an indicator for screening high-mechanical-performance BN structures. Hence, we performed an in-depth study on BN structures with a high density in the following investigation. Unless otherwise noted, each BN structure in this work is named as

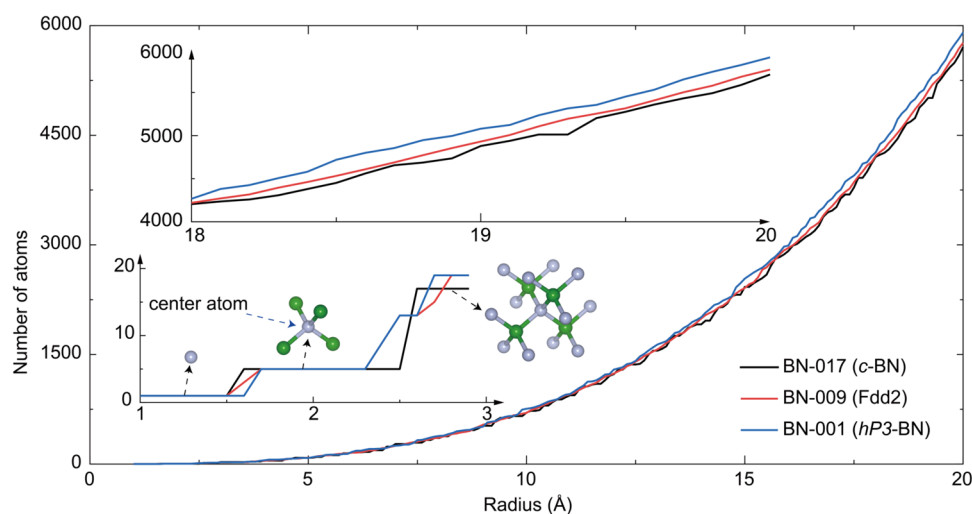


Figure 4. Superdense mechanisms of BN structures. Statistical analyses by counting the number of atoms within various spherical shells centered on each atom for BN-001 (*hP3*-BN) and BN-009 (*Fdd2*) compared to BN-017 (*c*-BN).

“BN-number (space group)” (Table S1). Among these 194 BN structures, 17 exhibit densities exceeding that of *c*-BN and were defined as superdense BN structures. We further investigated the thermodynamic stabilities of superdense BN structures by conducting AIMD simulations for 10 ps at room temperature (300 K). The simulations show that 15 structures from templates can maintain structural integrity (Figure 3), and 13 of them are newly found in this work. In the following investigation, we refer to structures that possess both mechanical and thermodynamic stability as stable structures, and we exclusively focus on these stable superdense BN structures.

Considering the mechanical anisotropy, the direction-dependent mechanical properties are also interesting. The mechanical anisotropy of BN-009 (*Fdd2*) (the ratio of the maximum and minimum Young’s modulus: $Y_{\max}/Y_{\min} = 2.9$) exceeds that of *c*-BN ($Y_{\max}/Y_{\min} = 1.3$), and BN-009 (*Fdd2*) has the highest recorded Y_{\max} (1175 GPa) that is 21% larger than that of *c*-BN (974 GPa). To the best of our knowledge, no other BN structures have been identified to have a higher Y_{\max} than BN-009 (*Fdd2*). Furthermore, the densest [BN-001 (*hP3*-BN)] and stiffest [BN-009 (*Fdd2*)] BN structures discovered from our template-based screening were investigated by uniaxial tensile tests along the direction of the maximum Young’s modulus. Tensile tests of BN-017 (*c*-BN) and BN-122 (*Pm3n*-BN with the highest tensile strength of 121 GPa reported in literature²³) were also performed for comparison (Figure S2). The results show that the tensile strengths for BN-017 (*c*-BN) and BN-122 (*Pm3n*-BN) in the Y_{\max} direction are 59 and 117 GPa, respectively, which are generally consistent with the literature reported values (55 and 121 GPa, respectively),^{20,23} while the tensile strength of BN-001 (*hP3*-BN) (172 GPa) and BN-009 (*Fdd2*) (126 GPa) significantly exceed the highest reported tensile strength of BN-122 (*Pm3n*-BN) (117 GPa). To summarize, these results demonstrate that our template-directed search has led to the discovery of the predicted stiffest BN structure [BN-009 (*Fdd2*)] and the predicted strongest BN structure [BN-001 (*hP3*-BN)].

Considering the correlations between the densities and the mechanical properties, an investigation of BN-001 (*hP3*-BN) and BN-009 (*Fdd2*) was conducted to elucidate the mechanisms for their higher densities than BN-017 (*c*-BN).

All these structures are tetrahedrally coordinated (sp^3 hybridization as shown in Figure 2). Despite their tetrahedral coordination, the tetrahedral structures of these BN variants are not identical. BN-001 (*hP3*-BN) and BN-009 (*Fdd2*) can be regarded as distorted structures compared to BN-017 (*c*-BN). This structural distortion is reflected in the atomic distribution. To probe the atomic distribution at various neighbor levels, we performed statistical analyses by counting the number of atoms within various spherical shells centered on each atom. As shown in Figure 4, within the shell radius range of 2.8–2.9 Å, BN-001 (*hP3*-BN) and BN-009 (*Fdd2*) accommodate 19 atoms, whereas BN-017 (*c*-BN) accommodates 17 atoms. As the shell radius increases, the difference in the number of atoms among these structures becomes more pronounced. In the range of 18–20 Å, BN-001 (*hP3*-BN) and BN-009 (*Fdd2*) exhibit a higher number of atoms compared to BN-017 (*c*-BN). This highlights the role of structural distortions in enhancing the density of these materials. As the radius grows, the density gap continues to increase, providing a clearer distinction between these structures. This mechanism is similar to analogous carbon structures (*hP3* carbon and diamond).⁵⁵

Additional Remarks on the Fabrication of BN Structures. The synthesis of materials is a key for applications. To synthesize BN structures, various methods can be employed, including high-temperature and high-pressure synthesis,^{14,54} atmospheric pressure synthesis,⁵⁶ temperature gradient method,⁵⁷ chemical vapor deposition method,⁵⁸ and physical vapor deposition method.⁵⁹ Each method has its advantages and limitations.¹² The choice of BN precursors significantly influences the resultant BN structures. For example, onion-like BN has been used as the precursor to synthesize nanotwinned *c*-BN,⁵⁴ and *h*-BN has been used as the precursor to synthesize *c*-BN and *w*-BN.^{14–16,52} O-BN has been predicted that it can be synthesized using BN nanotubes as the precursor.⁵² These results suggest that it is possible to synthesize new BN structures through low-density, low-dimensional BN structures, such as fullerene-like BN structures,⁶⁰ and amorphous structures.⁶¹ Our newly predicted BN structures exhibit excellent mechanical properties and hold great promise to be synthesized experimentally. These BN structures, along with their remarkable properties, show

promising potential for various technological fields.^{10,11,62–65} For example, BN-001 (*hP3*-BN) and BN-009 (*Fdd2*) exhibit fracture strains greater than 20%, making them suitable for applications in strain engineering and related fields. Moreover, the energy above hull is used to characterize the formability of a material. A low energy above hull usually indicates likely ease of synthesis for a material. Our calculated energies above hull of 194 BN structures are shown in Figure 1d and Table S1. It can be found that all the energies above hull for these BN structures from templates are below 1.4 eV/atom, and most of them are below 0.5 eV/atom, indicating their formability for applications. These results provide references for future BN syntheses.

CONCLUSIONS

In summary, we propose a template-directed searching strategy to accelerate the discovery of BN structures from complex energy landscapes. This search yields 171 unique BN structures with good mechanical stability. Among these structures, 32 BN structures have been computationally or experimentally fabricated in the literature, providing valuable support for our work. Meanwhile, the number of known mechanically stable BN structures has more than tripled, indicating that our template-directed search significantly extends the family of BN structures. Analyses of these structures show strong correlations between the densities and the mechanical properties. Most interestingly, 15 stable BN structures from templates have a density significantly higher than *c*-BN, and 13 of them are newly found, including the predicted densest and strongest BN-001 (*hP3*-BN), and the predicted stiffest BN-009 (*Fdd2*). Finally, the superdense mechanisms and possible synthesis of high-performance BN structures are discussed.

ASSOCIATED CONTENT

Supporting Information

The Supporting Information is available free of charge at <https://pubs.acs.org/doi/10.1021/acs.jpcc.4c08627>.

Highest Young's modulus (Y_{\max}) vs density (ρ) for mechanically stable BN structures from the template method, tensile stress–strain curves of BN structures stretched along the direction of highest Young's modulus, and raw data of calculations and relevant literature (PDF)

AUTHOR INFORMATION

Corresponding Author

Enlai Gao – Department of Engineering Mechanics, School of Civil Engineering, Wuhan University, Wuhan, Hubei 430072, China; orcid.org/0000-0003-1960-0260;
Email: enlaigao@whu.edu.cn

Authors

Yongheng Wang – Department of Engineering Mechanics, School of Civil Engineering, Wuhan University, Wuhan, Hubei 430072, China

Yongzhe Guo – Department of Engineering Mechanics, School of Civil Engineering, Wuhan University, Wuhan, Hubei 430072, China

Chunbo Zhang – Department of Engineering Mechanics, School of Civil Engineering, Wuhan University, Wuhan, Hubei 430072, China

Complete contact information is available at: <https://pubs.acs.org/10.1021/acs.jpcc.4c08627>

Author Contributions

[†]Y.W. and Y.G. contributed equally.

Notes

The authors declare no competing financial interest.

ACKNOWLEDGMENTS

We thank Prof. Zhisheng Zhao at Yanshan University for helpful discussions. This work is supported by the National Natural Science Foundation of China (Grant Nos. 12472107 and 12172261). The numerical calculations in this work are done on the supercomputing system in the Supercomputing Center of Wuhan University.

REFERENCES

- (1) Koziol, K.; Vilatela, J.; Moisala, A.; Motta, M.; Cuniff, P.; Sennett, M.; Windle, A. High-performance carbon nanotube fiber. *Science* **2007**, *318*, 1892–1895.
- (2) Xin, G.; Yao, T.; Sun, H.; Scott, S. M.; Shao, D.; Wang, G.; Lian, J. Highly thermally conductive and mechanically strong graphene fibers. *Science* **2015**, *349*, 1083–1087.
- (3) Telling, R. H.; Pickard, C. J.; Payne, M. C.; Field, J. E. Theoretical strength and cleavage of diamond. *Phys. Rev. Lett.* **2000**, *84*, 5160–5163.
- (4) Li, Y.; Hao, J.; Liu, H.; Lu, S.; Tse, J. S. High-energy density and superhard nitrogen-rich B-N compounds. *Phys. Rev. Lett.* **2015**, *115*, No. 105502.
- (5) Shao, Q.; Li, R.; Yue, Z.; Wang, Y.; Gao, E. Data-driven discovery and understanding of ultrahigh-modulus crystals. *Chem. Mater.* **2021**, *33*, 1276–1284.
- (6) Wentorf, R. H.; Devries, R. C.; Bundy, F. P. Sintered superhard materials. *Science* **1980**, *208*, 873–880.
- (7) Park, S.-T.; Han, J.; Keuneecke, M.; Lee, K. Mechanical and structural properties of multilayer *c*-BN coatings on cemented carbide cutting tools. *Int. J. Refract. Met. Hard Mater.* **2017**, *65*, 52–56.
- (8) Keuneecke, M.; Wiemann, E.; Weigel, K.; Park, S. T.; Bewilogua, K. Thick *c*-BN coatings – Preparation, properties and application tests. *Thin Solid Films* **2006**, *515*, 967–972.
- (9) Zhao, Z.; Xu, B.; Tian, Y. Recent advances in superhard materials. *Annu. Rev. Mater. Res.* **2016**, *46*, 383–406.
- (10) Monteiro, S. N.; Skury, A. L. D.; de Azevedo, M. G.; Bobrovitchii, G. S. Cubic boron nitride competing with diamond as a superhard engineering material – an overview. *J. Mater. Res. Technol.* **2013**, *2*, 68–74.
- (11) Sharma, V.; Kagada, H. L.; Jha, P. K.; Śpiewak, P.; Kurzydłowski, K. J. Thermal transport properties of boron nitride based materials: A review. *Renewable Sustainable Energy Rev.* **2020**, *120*, No. 109622.
- (12) Izyumskaya, N.; Demchenko, D. O.; Das, S.; Özgür, Ü.; Avrutin, V.; Morkoç, H. Recent development of boron nitride towards electronic applications. *Adv. Electron. Mater.* **2017**, *3*, No. 1600485.
- (13) Fan, Q.; Ai, X.; Song, Y.; Yu, X.; Yun, S. Two novel large-cell boron nitride polymorphs. *Diamond Relat. Mater.* **2022**, *126*, No. 109046.
- (14) Wentorf, R. H. Cubic form of boron nitride. *J. Chem. Phys.* **1957**, *26*, 956.
- (15) Wentorf, R. H. Synthesis of the cubic form of boron nitride. *J. Chem. Phys.* **1961**, *34*, 809–812.
- (16) Bundy, F. P.; Wentorf, R. H. Direct transformation of hexagonal boron nitride to denser forms. *J. Chem. Phys.* **1963**, *38*, 1144–1149.
- (17) Xu, Y. N.; Ching, W. Y. Calculation of ground-state and optical properties of boron nitrides in the hexagonal, cubic, and wurtzite structures. *Phys. Rev. B* **1991**, *44*, 7787–7798.

- (18) Furthmüller, J.; Hafner, J.; Kresse, G. *Ab initio* calculation of the structural and electronic properties of carbon and boron nitride using ultrasoft pseudopotentials. *Phys. Rev. B* **1994**, *50*, 15606–15622.
- (19) Mirkarimi, P. B.; Medlin, D. L.; McCarty, K. F.; Dibble, D. C.; Clift, W. M.; Knapp, J. A.; Barbour, J. C. The synthesis, characterization, and mechanical properties of thick, ultrahard cubic boron nitride films deposited by ion-assisted sputtering. *J. Appl. Phys.* **1997**, *82*, 1617–1625.
- (20) Zhang, R. F.; Veprek, S.; Argon, A. S. Anisotropic ideal strengths and chemical bonding of wurtzite BN in comparison to zincblende BN. *Phys. Rev. B* **2008**, *77*, No. 172103.
- (21) Deura, M.; Kutsukake, K.; Ohno, Y.; Yonenaga, I.; Taniguchi, T. Nanoindentation measurements of a highly oriented wurtzite-type boron nitride bulk crystal. *Jpn. J. Appl. Phys.* **2017**, *56*, No. 030301.
- (22) Kuzubov, A. A.; Tikhonova, L. V.; Fedorov, A. S. *Ab initio* investigation of a new boron nitride allotrope. *Phys. Status Solidi B* **2014**, *251*, 1282–1285.
- (23) Xiong, C.; Shi, J.; Zhou, A.; Cai, Y. A comparative investigation of sp^3 -hybridized $Pm3n$ -BN and sc - $B_{12}N_{12}$ based on density functional theory (DFT). *Mater. Today Commun.* **2020**, *25*, No. 101582.
- (24) Wang, Y.; Lv, J.; Zhu, L.; Ma, Y. Crystal structure prediction via particle-swarm optimization. *Phys. Rev. B* **2010**, *82*, No. 094116.
- (25) Šimůnek, A. How to estimate hardness of crystals on a pocket calculator. *Phys. Rev. B* **2007**, *75*, No. 172108.
- (26) Šimůnek, A.; Vackář, J. Hardness of covalent and ionic crystals: First-principle calculations. *Phys. Rev. Lett.* **2006**, *96*, No. 085501.
- (27) Zhang, X.; Wang, Y.; Lv, J.; Zhu, C.; Li, Q.; Zhang, M.; Li, Q.; Ma, Y. First-principles structural design of superhard materials. *J. Chem. Phys.* **2013**, *138*, No. 114101.
- (28) Zhou, R.; Dai, J.; Cheng Zeng, X. Structural, electronic and mechanical properties of sp^3 -hybridized BN phases. *Phys. Chem. Chem. Phys.* **2017**, *19*, 9923–9933.
- (29) Hoffmann, R.; Kabanov, A. A.; Golov, A. A.; Proserpio, D. M. *Homo citans* and carbon allotropes: For an ethics of citation. *Angew. Chem., Int. Ed.* **2016**, *55*, 10962–10976.
- (30) Xiong, M.; Yuan, Z.; Mao, F.; Wang, X.; Jin, D.; Zhang, Q.; Yu, D.; Wang, C.; Wei, S. Superhard $B_{28}N_{32}$ with three-dimensional metallicity: First-principles prediction. *Comput. Mater. Sci.* **2021**, *188*, No. 110121.
- (31) Hautier, G.; Fischer, C.; Ehlacher, V.; Jain, A.; Ceder, G. Data mined ionic substitutions for the discovery of new compounds. *Inorg. Chem.* **2011**, *50*, 656–663.
- (32) Kresse, G.; Furthmüller, J. Efficiency of *ab-initio* total energy calculations for metals and semiconductors using a plane-wave basis set. *Comput. Mater. Sci.* **1996**, *6*, 15–50.
- (33) Perdew, J. P.; Burke, K.; Ernzerhof, M. Generalized gradient approximation made simple. *Phys. Rev. Lett.* **1996**, *77*, 3865.
- (34) Monkhorst, H. J.; Pack, J. D. Special points for Brillouin-zone integrations. *Phys. Rev. B* **1976**, *13*, 5188–5192.
- (35) Andersen, H. C. Molecular dynamics simulations at constant pressure and/or temperature. *J. Chem. Phys.* **1980**, *72*, 2384–2393.
- (36) Wang, Y.; Zhang, C.; Guo, Y.; Gao, E. Template directed *ab initio* search for superdense, ultrahard carbon structures. Unpublished, 2024.
- (37) Fan, Q.; Li, W.; Wu, N.; Zhao, Y.; Song, Y.; Yu, X.; Yun, S. Study of the novel boron nitride polymorphs: First-principles calculations and machine learning. *Chin. J. Phys.* **2024**, *89*, 1908–1919.
- (38) Fan, Q.; Min, G.; Liu, L.; Zhao, Y.; Yu, X.; Yun, S. Accelerate the design of new superhard carbon allotropes in $Pca2_1$ space group: High-throughput screening and machine learning strategies. *Diamond Relat. Mater.* **2024**, *143*, No. 110928.
- (39) Jia, M.; Fan, Q.; Gao, D.; Pang, Q.; Yun, S. High-throughput screening of novel silicon allotropes in $Fmmm$ phase with unique electronic physical performances and potential photovoltaic applications. *Comput. Mater. Sci.* **2025**, *248*, No. 113613.
- (40) Min, G.; Wei, W.; Fan, Q.; Wan, T.; Ye, M.; Yun, S. High-throughput exploration of stable semiconductors using deep learning and density functional theory. *Mater. Sci. Semicond. Process.* **2025**, *188*, No. 109150.
- (41) Fan, Q.; Liu, H.; Ren, C.; Yun, S.; Schwingenschlögl, U. High-throughput design of three-dimensional carbon allotropes with $Pmma$ space group. *Mater. Today Adv.* **2024**, *22*, No. 100486.
- (42) Fan, Q.; Wu, J.; Zhao, Y.; Song, Y.; Yun, S. High-throughput calculation screening for new silicon allotropes with monoclinic symmetry. *IUCrJ* **2023**, *10*, 464–474.
- (43) Zhang, B.; He, Y.; Gao, H.; Wang, X.; Liu, J.; Xu, H.; Wang, L.; He, X. Unraveling the doping mechanisms in lithium iron phosphate. *Energy Mater.* **2022**, *2*, No. 200022.
- (44) Curtarolo, S.; Setyawan, W.; Hart, G. L. W.; Jahnatek, M.; Chepulskii, R. V.; Taylor, R. H.; Wang, S.; Xue, J.; Yang, K.; Levy, O.; et al. Aflow: An automatic framework for high-throughput materials discovery. *Comput. Mater. Sci.* **2012**, *58*, 218–226.
- (45) Ashton, M.; Paul, J.; Sinnott, S. B.; Hennig, R. G. Topology-scaling identification of layered solids and stable exfoliated 2D materials. *Phys. Rev. Lett.* **2017**, *118*, No. 106101.
- (46) Le Page, Y.; Saxe, P. Symmetry-general least-squares extraction of elastic data for strained materials from *ab initio* calculations of stress. *Phys. Rev. B* **2002**, *65*, No. 104104.
- (47) Hill, R. The elastic behaviour of a crystalline aggregate. *Proc. Phys. Soc. A* **1952**, *65*, 349–354.
- (48) Chen, X.-Q.; Niu, H.; Li, D.; Li, Y. Modeling hardness of polycrystalline materials and bulk metallic glasses. *Intermetallics* **2011**, *19*, 1275–1281.
- (49) Gao, F.; He, J.; Wu, E.; Liu, S.; Yu, D.; Li, D.; Zhang, S.; Tian, Y. Hardness of covalent crystals. *Phys. Rev. Lett.* **2003**, *91*, No. 015502.
- (50) Yao, H.; Ouyang, L.; Ching, W. *Ab initio* calculation of elastic constants of ceramic crystals. *J. Am. Ceram. Soc.* **2007**, *90*, 3194–3204.
- (51) Fan, Q.-Y.; Li, C.; Zhao, Y.; Song, Y.; Yun, S. A novel superhard boron nitride polymorph with monoclinic symmetry. *Commun. Theor. Phys.* **2022**, *74*, No. 065701.
- (52) Huang, Q.; Yu, D.; Zhao, Z.; Fu, S.; Xiong, M.; Wang, Q.; Gao, Y.; Luo, K.; He, J.; Tian, Y. First-principles study of O-BN: A sp^3 -bonding boron nitride allotrope. *J. Appl. Phys.* **2012**, *112*, No. 053518.
- (53) Huang, Q.; Yu, D.; Xu, B.; Hu, W.; Ma, Y.; Wang, Y.; Zhao, Z.; Wen, B.; He, J.; Liu, Z.; Tian, Y. Nanotwinned diamond with unprecedented hardness and stability. *Nature* **2014**, *510*, 250–253.
- (54) Tian, Y.; Xu, B.; Yu, D.; Ma, Y.; Wang, Y.; Jiang, Y.; Hu, W.; Tang, C.; Gao, Y.; Luo, K.; et al. Ultrahard nanotwinned cubic boron nitride. *Nature* **2013**, *493*, 385–388.
- (55) Zhu, Q.; Oganov, A. R.; Salvadó, M. A.; Pertierra, P.; Lyakhov, A. O. Denser than diamond: *Ab initio* search for superdense carbon allotropes. *Phys. Rev. B* **2011**, *83*, No. 193410.
- (56) Kubota, Y.; Watanabe, K.; Tsuda, O.; Taniguchi, T. Deep ultraviolet light-emitting hexagonal boron nitride synthesized at atmospheric pressure. *Science* **2007**, *317*, 932–934.
- (57) Taniguchi, T.; Yamaoka, S. Spontaneous nucleation of cubic boron nitride single crystal by temperature gradient method under high pressure. *J. Cryst. Growth* **2001**, *222*, 549–557.
- (58) Yu, J.; Matsumoto, S. Synthesis of thick and high quality cubic boron nitride films by r.f. bias assisted d.c. jet plasma chemical vapor deposition. *Diamond Relat. Mater.* **2004**, *13*, 1704–1708.
- (59) Hofsäss, H.; Eyhusen, S.; Ronning, C. On the mechanisms of cubic boron nitride film growth. *Diamond Relat. Mater.* **2004**, *13*, 1103–1110.
- (60) Jensen, F.; Toftlund, H. Structure and stability of C_{24} and $B_{12}N_{12}$ isomers. *Chem. Phys. Lett.* **1993**, *201*, 89–96.
- (61) Taniguchi, T.; Kimoto, K.; Tansho, M.; Horiuchi, S.; Yamaoka, S. Phase transformation of amorphous boron nitride under high pressure. *Chem. Mater.* **2003**, *15*, 2744–2751.
- (62) Fan, Q.-Y.; Wu, N.; Chen, S.; Jiang, L.; Zhang, W.; Yu, X.; Yun, S. $P2_13$ BN: A novel large-cell boron nitride polymorph. *Commun. Theor. Phys.* **2021**, *73*, No. 125701.

(63) Fan, Q.; Zhou, H.; Zhao, Y.; Yun, S. Predicting a novel two-dimensional BN material with a wide band gap. *Energy Mater.* **2022**, *2*, No. 200022.

(64) Fan, Q.; Zhao, R.; Zhao, Y.; Song, Y.; Yun, S. Two new BN polymorphs with wide-bandgap. *Diamond Relat. Mater.* **2022**, *130*, No. 109410.

(65) Fan, Q.; Wu, N.; Yang, R.; Zhang, W.; Yu, X.; Yun, S. All sp^2 hybridization BN polymorphs with wide bandgap. *J. Appl. Phys.* **2022**, *131*, No. 055703.